An inversion formula for the exponential Radon transform in spatial domain with variable focal-length fan-beam collimation geometry

Junhai Wen
Department of Biomedical Engineering, Beijing Institute of Technology, Beijing, 100081, China and Department of Radiology, State University of New York, Stony Brook, New York 11794

Zhengrong Liang
Department of Radiology, State University of New York, Stony Brook, New York 11794

(Received 18 July 2005; revised 6 January 2006; accepted for publication 10 January 2006; published 27 February 2006)

Inverting the exponential Radon transform has a potential use for SPECT (single photon emission computed tomography) imaging in cases where a uniform attenuation can be approximated, such as in brain and abdominal imaging. Tretiak and Metz derived in the frequency domain an explicit inversion formula for the exponential Radon transform in two dimensions for parallel-beam collimator geometry. Progress has been made to extend the inversion formula for fan-beam and varying focal-length fan-beam (VFF) collimator geometries. These previous fan-beam and VFF inversion formulas require a spatially variant filtering operation, which complicates the implementation and imposes a heavy computing burden. In this paper, we present an explicit inversion formula, in which a spatially invariant filter is involved. The formula is derived and implemented in the spatial domain for VFF geometry (where parallel-beam and fan-beam geometries are two special cases). Phantom simulations mimicking SPECT studies demonstrate its accuracy in reconstructing the phantom images and efficiency in computation for the considered collimator geometries. © *2006 American Association of Physicists in Medicine*. [DOI: 10.1118/1.2170596]

Key words: exponential Radon transform, spatial domain, variable focal-length fan-beam geometry

I. INTRODUCTION

Single photon emission computed tomography (SPECT) is a functional imaging modality which aims to reconstruct an image of the uptake distribution within the tissues or organs of radiopharmaceutical or radiotracer, which is injected intravenously into the patient. The reconstruction is based on measurements of radiation emitted from the radiotracer. Because of photoelectric absorption and Compton scattering, the emitted γ photons are attenuated inside the body before arriving at the detector. Quantitative reconstruction of the radiotracer concentration at any location inside the body requires accurate compensation for the attenuation. Mathematically this is represented as an inversion of the attenuated Radon transform.[1] Inverting this transform has been a research topic for many years.[2] Recently an explicit inversion formula for the transform in two dimensions for parallel-beam collimator geometry was derived by Novikov[3] in a form similar to filtered backprojection.[4] The derivation was then simplified in Ref. 5 and implemented in Ref. 6. Thereafter, extension of the inversion formula to fan-beam,[7–9] varying focal-length fan-beam (VFF),[9,10] and cone-beam[11] geometries has been attempted by various strategies. Although it is accurate for the extended inversion, the ray-driven strategy[7,10] is computationally expensive.[12] While the coordinate transform strategy in Refs. 8 and 11 offers a close-form solution under some assumptions, it is limited to the fixed focal-length geometries. The functional transform strategy in Ref. 9 has shown efficacy in both reconstruction accuracy and computation speed and is worth further evaluation. Despite their preliminary natures, these extension attempts are expected to attract more research interests, because fan-beam, VFF, and cone-beam geometries have the potential to improve counting statistics and imaging resolution.[13–15]

If the attenuation of the object, such as the head with a completed skull enclosure, can be approximated as uniform,[16] the attenuated Radon transform reduces or simplifies to the exponential Radon transform.[17] Tretiak and Metz[17] derived in the frequency domain an explicit inversion formula for this transform in two dimensions for parallel-beam geometry. (Alternative inversion formulas with different presentation or implementation strategies can be seen in Refs. 18–21). Theoretically, the Tretiak and Metz inversion formula can be deduced from the Novikov formula by assuming the attenuation coefficient to be a constant.[6] Extension of the Tretiak and Metz inversion from parallel- to fan-beam geometry was made by Weng *et al.*[22] with the Cartesian coordinate transformation in the spatial domain. In their extended formula, a filter function has to be used which varies according to each reconstruction point. Therefore, implementation of their extended formula has to perform a spatially variant filtering operation by a point-by-point fashion, which is computationally intensive. You *et al.*[23] presented a Cormack-type reconstruction framework for the exponential Radon transform based on harmonic decomposition for parallel-beam, fan-beam, and VFF geometries. The Cormack-type reconstruction framework is generally applicable to all these three

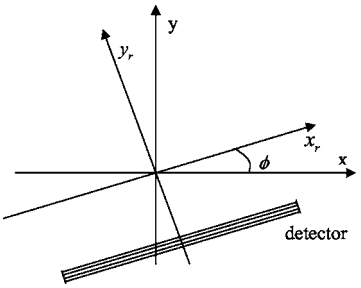

FIG. 1. The rotated coordinate system.

collimator geometries, but it does not give an explicit reconstruction formula, and its presentation and implementation in the frequency space are very complicated.

In this paper, we derive an explicit inversion formula using the polar coordinate transformation, instead of the Cartesian coordinate transformation, in the spatial domain for the exponential Radon transform for parallel-beam, fan-beam, and VFF collimator geometries. Our extended inversion formula involves a spatially invariant filter, rather than a spatially variant one, and therefore has the advantages of simplicity in implementation and efficiency in computation.

II. REVIEW OF A SPATIAL-DOMAIN INVERSION FORMULA FOR THE EXPONENTIAL RADON TRANSFORM IN PARALLEL-BEAM COLLIMATOR GEOMETRY

For presentation of tomographic imaging methodologies, a rotated coordinate system (x_r, y_r) is usually introduced (see Fig. 1),

$$x_r = x\cos\phi + y\sin\phi,$$

$$y_r = -x\sin\phi + y\cos\phi. \tag{1}$$

The measured projection data at angle ϕ can be expressed as

$$g_\phi(x_r) = \int_{-\infty}^{\infty} \exp[-(D_\phi a_\phi)(x_r, y_r)] f_\phi(x_r, y_r) dy_r, \tag{2}$$

where $f_\phi(x_r, y_r)$ denotes the radiotracer distribution $f(x, y)$ in the rotated coordinate system which is to be reconstructed and $a_\phi(x_r, y_r)$ represents the attenuation coefficient map (which is assumed as uniform in this paper) of the body in the rotated coordinate system. Note that $g_\phi(x_r)$ is the projection datum at position x_r with projection angle ϕ. The operation $D_\phi a_\phi(x_r, y_r)$ on the attenuation map in Eq. (2) is called the divergent beam transform[5] and is expressed, in the case of uniform attenuation, by

$$(D_\phi a_\phi)(x_r, y_r) = D_\phi\{a_\phi(x_r, y_r)\} = \int_{\text{detector}}^{y_r} \mu dy'_r, \tag{3}$$

where μ is a constant attenuation coefficient.

In SPECT, the emitted gamma photons inside the body are attenuated before arriving at the detector, so

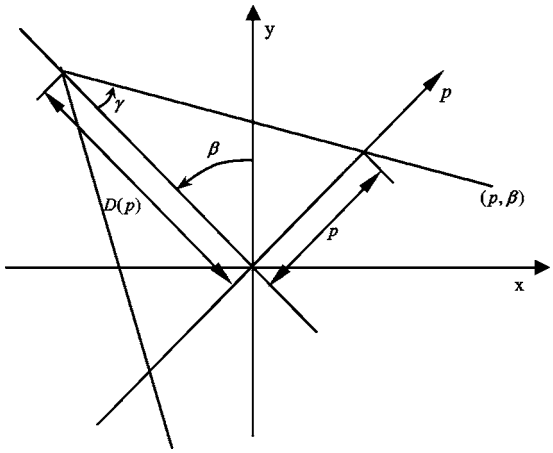

FIG. 2. The VFF collimator geometry.

$\exp[-(D_\phi a_\phi)(x_r, y_r)]$ is the attenuation of gamma photons emitted from point (x_r, y_r) before they arrive at the detector with angle of ϕ. Define

$$B_\phi(x_r, y_r) = \exp\left(\int_{\text{detector}}^{0} \mu dy'_r\right), \tag{4}$$

then the exponential Radon transform can be expressed as[17]

$$P_\mu f(x_r, \phi) = B_\phi(x_r, y_r) g_\phi(x_r) = \int_{-\infty}^{\infty} f_\phi(x_r, y_r) e^{-\mu y_r} dy_r. \tag{5}$$

An inversion formula for the exponential Radon transform in parallel-beam collimator geometry can be expressed, in the spatial domain, as

$$f(x,y) = \frac{1}{2}\int_0^{2\pi} e^{\mu y_r} \int_{-\infty}^{\infty} h(x_r - x'_r) P_\mu f(x'_r, \phi) dx'_r d\phi, \tag{6}$$

where $h(x_r)$ is a filter function, whose discrete format can be expressed, see Ref. 22, as

$$h(n) = \begin{cases} \dfrac{1}{4} - \dfrac{\mu^2}{4\pi^2} & n = 0 \\ \dfrac{-\mu\sin(n\mu)}{2\pi^2 n} + \dfrac{1-\cos(n\mu)}{2\pi^2 n^2} & n = \text{even} \\ \dfrac{-\mu\sin(n\mu)}{2\pi^2 n} - \dfrac{1+\cos(n\mu)}{2\pi^2 n^2} & n = \text{odd} \end{cases}. \tag{7}$$

III. A SPATIAL-DOMAIN INVERSION FORMULA FOR THE EXPONENTIAL RADON TRANSFORM IN VARYING FOCAL-LENGTH FAN-BEAM COLLIMATOR GEOMETRY

In a VFF collimator system, the focal length of projection rays varies according to the distance from a position on the collimator surface to the center of the collimator,[13,14] see Fig. 2. Any ray (p, β) in the VFF collimator geometry can be seen as a ray (x_r, ϕ) in the parallel-beam geometry of Fig. 1. Let $D(p)$ be the focal length for detector bin at position p, see Fig. 2.

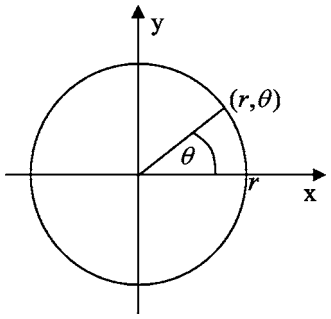

FIG. 3. The polar coordinates.

The relation between these two detector geometries is

$$\phi=\beta+\gamma=\beta+\arctan\frac{p}{D(p)},\quad x_r=p\cos\gamma=\frac{pD(p)}{\sqrt{D^2(p)+p^2}}. \tag{8}$$

In Ref. 22, Weng *et al.* derived a fan-beam inversion formula for the exponential Radon transform, where the Cartesian coordinates of Fig. 2 (for fixed focal length) were used. Because of the existence of the exponential items in Eq. (8), it is not trivial to find a relationship between the nonparallel rays in each view in the Cartesian coordinates for image reconstruction. So a filter function in their formula has to be implemented as a spatially varying operation on each reconstruction position, i.e., a filtering operation by a point-by-point manner, which can be computationally intensive.

In this work, we use the polar coordinates (see Fig. 3) to derive an explicit inversion formula for the exponential Radon transform in VFF collimator geometry which is also applicable to parallel-beam and fan-beam geometries. This inversion formula can be implemented directly in the spatial domain, and any filter function in the formula does not need to be implemented by a point-by-point manner, because of its spatial invariance.

For any point (x,y) in the Cartesian coordinates or (r,θ) in the polar coordinates, its position in the rotated coordinate system with a rotated angle ϕ is (x_r,y_r), and

$$x_r=r\cos(\theta-\phi)\quad y_r=r\sin(\theta-\phi). \tag{9}$$

In parallel-beam geometry, there is

$$\begin{aligned}
f(x,y)&=f(r,\theta)\\
&=\int_0^{2\pi}e^{\mu r\sin(\theta-\phi)}\int_{-\infty}^{\infty}h[r\cos(\theta-\phi)-x_r]\\
&\quad\times P_\mu f(x_r,\phi)d\phi dx_r\\
&=\int_{-\infty}^{\infty}dx_r\int_0^{2\pi}e^{\mu r\sin(\theta-\phi)}h[r\cos(\theta-\phi)-x_r]\\
&\quad\times P_\mu f(x_r,\phi)d\phi\\
&=\int_{-\infty}^{\infty}dx_r\int_0^{2\pi}e^{\mu r\sin(\theta-\theta')}h[r\cos(\theta-\theta')-x_r]\\
&\quad\times P_\mu f(x_r,\theta')d\theta'\\
&=\int_{-\infty}^{\infty}dx_r\int_0^{2\pi}h_e(\theta-\theta')P_\mu f(x_r,\theta')d\theta'\\
&=\int_{-\infty}^{\infty}dx_r\int_0^{2\pi}h_e(\phi-\phi')P_\mu f(x_r,\phi')d\phi',
\end{aligned} \tag{10}$$

where

$$h_e(\theta)=e^{\mu r\sin(\theta)}h[r\cos(\theta)-x_r]. \tag{11}$$

In VFF collimator geometry, the differential relationship for the coordinate change is

$$dx_r d\phi=|J|dpd\beta, \tag{12}$$

where the Jacobian $|J|$ is given by

$$|J|=\begin{vmatrix}\partial x_r/\partial p & \partial x_r/\partial\beta\\ \partial\phi/\partial p & \partial\phi/\partial\beta\end{vmatrix}=\frac{D^3(p)+p^3D'(p)}{\sqrt{(D^2(p)+p^2)^3}}. \tag{13}$$

Substituting Eq. (8) into Eq. (10), we can obtain the VFF inversion or reconstruction formula

$$\begin{aligned}
f(x,y)=f(r,\theta)&=\int_{-\infty}^{\infty}dx_r\int_0^{2\pi}e^{\mu r\sin(\theta-\phi)}h[r\cos(\theta-\phi)-x_r]P_\mu f(x_r,\phi)d\phi\\
&=\int_{-\infty}^{\infty}\int_0^{2\pi}e^{\mu r\sin\left[\theta-\beta-\arctan\left(\frac{p}{D(p)}\right)\right]}h\left\{r\cos\left[\theta-\beta-\arctan\left(\frac{p}{D(p)}\right)\right]-\frac{pD(p)}{\sqrt{D^2(p)+p^2}}\right\}P_\mu f(p,\beta)\frac{D^3(p)+p^3D'(p)}{\sqrt{[D^2(p)+p^2]^3}}d\beta dp\\
&=\int_{-\infty}^{\infty}\int_0^{2\pi}e^{\mu r\sin\left[\theta-\theta'-\arctan\left(\frac{p}{D(p)}\right)\right]}h\left\{r\cos\left[\theta-\theta'-\arctan\left(\frac{p}{D(p)}\right)\right]-\frac{pD(p)}{\sqrt{D^2(p)+p^2}}\right\}P_\mu f(p,\theta')\frac{D^3(p)+p^3D'(p)}{\sqrt{[D^2(p)+p^2]^3}}d\theta' dp\\
&=\int_{-\infty}^{\infty}\int_0^{2\pi}e^{\mu r\sin\left[\beta-\beta'-\arctan\left(\frac{p}{D(p)}\right)\right]}h\left\{r\cos\left[\beta-\beta'-\arctan\left(\frac{p}{D(p)}\right)\right]-\frac{pD(p)}{\sqrt{D^2(p)+p^2}}\right\}P_\mu f(p,\beta')\frac{D^3(p)+p^3D'(p)}{\sqrt{[D^2(p)+p^2]^3}}d\beta' dp\\
&=\int_{-\infty}^{\infty}\int_0^{2\pi}h_e(\beta-\beta')P_\mu f(p,\beta')\frac{D^3(p)+p^3D'(p)}{\sqrt{[D^2(p)+p^2]^3}}d\beta' dp,
\end{aligned} \tag{14}$$

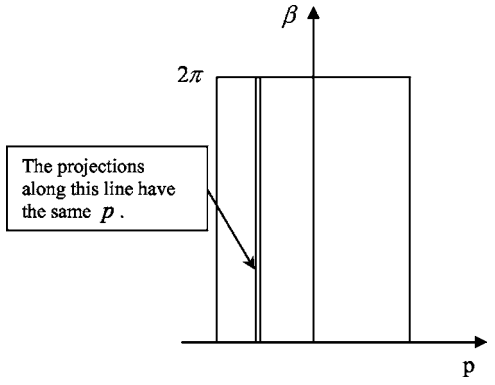

FIG. 4. Projections in the sinogram domain.

where

$$h_e(\beta) = e^{\mu r \sin\left[\beta - \arctan\left(\frac{p}{d(p)}\right)\right]} h\left\{ r\cos\left[\beta - \arctan\left(\frac{p}{D(p)}\right)\right] - \frac{pD(p)}{\sqrt{D^2(p)+p^2}}\right\}. \quad (15)$$

From Eqs. (14) and (15), we can see when r is fixed, $h_e(\beta)$ depends only on p. In the sinogram domain (see Fig. 4), the projections along the line parallel to the β axis have the same p value and, therefore, they can be convoluted by the same filter $h_e(\beta)$. So image reconstruction by the inversion formula should not be implemented view-by-view (i.e., β from 0 to 2π) as most previously reported reconstruction procedures do. Instead it should be implemented distance-by-distance (i.e., p from $-\infty$ to ∞).

Our inversion reconstruction procedure for the exponential Radon transform in VFF collimator geometry can be summarized as

1. Compute the filter function $h_e(\beta)$ with respect to the variables β and p.
2. Compute the convolution of $h_e(\beta)$ with corresponding projection data $P_\mu f(p,\beta)$.
3. Back project with respect to the variable p, then $f(r,\theta)$ is obtained.
4. Finally, transform the polar coordinate expression $f(r,\theta)$ to the Cartesian coordinate expression $f(x,y)$. In the implementation of the coordinate transformation, a linear interpolation was used to convert the reconstructed image from the polar coordinates to the Cartesian coordinates.

IV. RESULTS

Computer simulation studies were performed to verify the derived inversion formula using the Shepp-Logan mathematical phantom with uniform attenuation on an image of 128×128 pixel array size, see Fig. 5(a). The constant attenuation coefficient μ for the emission phantom was assumed 0.02/pixel. Attenuated projection data were simulated by a line integral through the phantom using parallel-beam, fan-beam, and VFF collimator geometries, respectively. For each collimator geometry, a total of 128 projections were generated evenly spaced on a circular orbit. Each projection had 128 bins uniformly spaced.

Figure 5 shows the reconstructed images of the emission phantom by the presented inversion reconstruction formula for parallel-beam, fan-beam, and VFF collimator geometries. Picture 5(a) shows the radiotracer emission phantom. Its uniform attenuation map can be generated by setting all the pixels (inside the outer elliptical boundary) to have a constant μ value. Picture 5(b) shows the reconstructed image without attenuation compensation for parallel-beam geometry [i.e., setting the μ value as zero and focal length to be very large (or infinite) for the VFF inversion formula of Eqs. (14) and (15)]. The attenuation effect of a lower reconstructed emission density in the central region is clearly seen because of the absence of compensation for the attenuation in the projection data. The elliptical boundary is blurred in some degree due to the limited data sampling rate. Picture 5(c) is the reconstructed image from the parallel-beam projections, where the attenuation effect was compensated, i.e., the uniform emission density in the phantom was recovered across the field-of-view (FOV) in the reconstructed image. There are some small streak artifacts in the central region of the reconstructed image. This may be due to the limited sampling rate and will be investigated later. Picture 5(d) shows the reconstructed image from the fan-beam projections with the focal length $D=300$ pixel units [i.e., setting the focal length function in Eqs. (14) and (15) as a constant]. This focal length is the shortest one for the phantom without truncation. Picture 5(e) shows the reconstructed image from the VFF projections with the focal length function $D(p)=100+10|p|$ pixel units. The focal length function varies from very short (i.e., a length of 100 pixel units, which is slightly shorter than the FOV dimension of 128 pixel units) for the central region to a longer one to ensure no truncation for the phantom. Both the fan-beam and VFF reconstructions show a similar quality as the parallel-beam result, reflecting an accurate reconstruction of the phantom. This indicates the correctness of the inversion formula in theory.

In the above experiment, a linear interpolation was used to convert the reconstructed image from the polar coordinates to the Cartesian coordinates. Due to the nonuniform sampling nature of fan-beam and VFF geometries across the object, a linear interpolation may not be sufficient to maintain the accuracy from the polar coordinates to the Cartesian coordinates. To observe the insufficiency of the linear interpolation, we performed another experiment with different focal lengths in the fan-beam geometry. Figure 6 shows the reconstruction results with the chosen different focal lengths in the fan-beam geometry. Picture (a) shows the result from focal length of $D=200$ pixel units, (b) of $D=300$ pixel units, (c) of $D=400$ pixel units, and (d) of $D=500$ pixel units. From these results, we can see that when the focal length is short (e.g., $D=200$ pixel units), the center of the reconstructed image is fine, but the periphery of the reconstructed image is blurred. This may be caused by the uneven data sampling in the fan-beam geometry and the use of a spatially

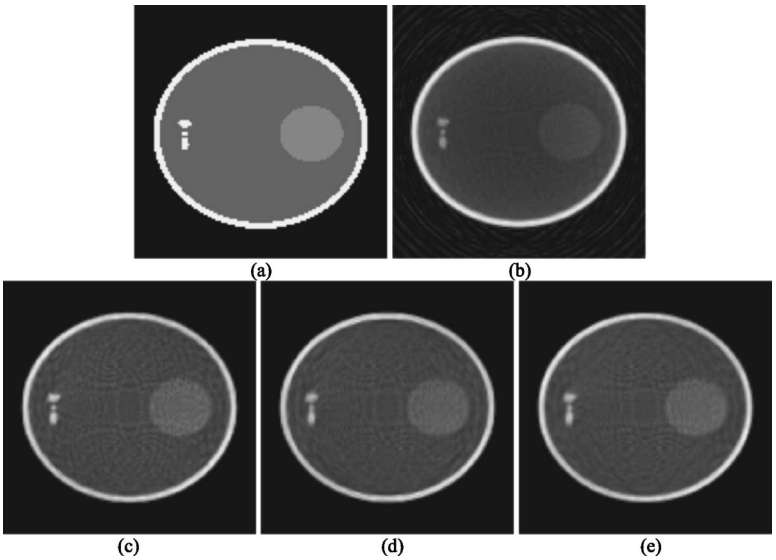

FIG. 5. Reconstruction results of different collimator geometries. Picture (a) is the phantom, (b) is the reconstructed image without attenuation compensation for the parallel-beam projections, (c) is the reconstructed image from the parallel-beam projections with attenuation compensation, (d) is the reconstructed image from the fan-beam projections with the focal length of $D=300$ pixel units, and (e) is the reconstructed image from the VFF projections with the focal length function of $D(p)=100+10|p|$ pixel units.

invariant linear interpolation that convert the reconstructed image from the polar coordinates to the Cartesian coordinates. Further investigation on the spatially variant data sampling and the use of an appropriate interpolation strategy is needed.

In addition to the noise-free simulation study above, a noise simulation was also performed, in which Poisson noise was added to the fan-beam and VFF projection data, respectively. The reconstruction procedures were repeated for these two collimator geometries. Figure 7 shows their reconstruction results and the corresponding profiles drawn along the central horizontal line across the images.

The reconstructions in the noise simulation show the same randomness as that in the projection data, without any noise-induced structural artifacts. This is expected because the inversion described here reconstructs an unbiased estimate of the mean emission density plus textured zero-mean noise that results from propagation of Poisson data noise through the inversion process.

In summary, both the noise-free and the noise simulation results demonstrate the accuracy and robustness of the presented inversion reconstruction formula for the exponential Radon transform in parallel-beam, fan-beam, and VFF collimator geometries.

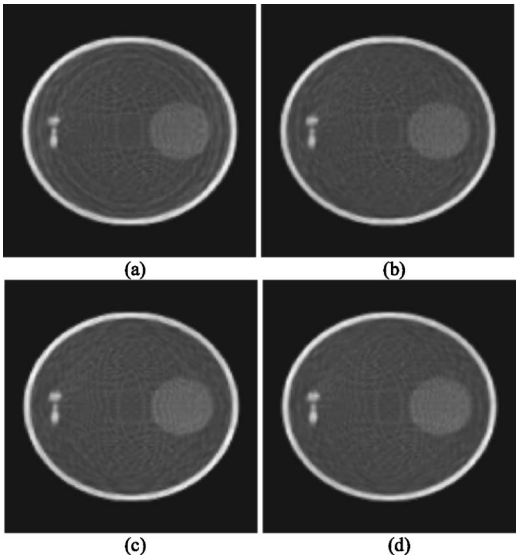

FIG. 6. Reconstruction results with different focal lengths in the fan-beam geometry. Picture (a) shows the result from a focal length of $D=200$ pixel units, (b) of $D=300$ pixel units, (c) of $D=400$ pixel units, and (d) of $D=500$ pixel units.

V. CONCLUSIONS AND DISCUSSIONS

In this paper, we derived an explicit inversion formula for the exponential Radon transform in the spatial domain. The derivation is based on the VFF collimator geometry and is generally applicable to the parallel-beam and fan-beam collimators. Because of the use of the polar coordinate transformation, instead of the Cartesian coordinate transformation,[22] the derived inversion formula does not need to perform a spatially variant filtering operation in a point-by-point manner across the FOV. This is a major advantage, as compared to the previous work,[22] in addition to the extension from fan-beam to VFF collimator geometry. Compared to the previous work,[23] the derivation of the presented formula is more explicit or less complex, and its implementation is more straightforward in the spatial domain, rather than in the frequency space. Phantom simulation results, in both noise-free and noise cases, have demonstrated the accuracy and robustness of the presented formula in reconstructing the phantom images for the three collimator geometries.

Because of the use of the polar coordinate transformation, the image is initially reconstructed in the polar coordinates. An interpolation from the polar coordinates to the Cartesian coordinates is needed. This needed interpolation has a similar effect as the interpolation of nonparallel beam projection data to parallel-beam geometry projection data, followed by a parallel-beam geometry reconstruction algorithm.[24] While most previous work seems to prefer a coordinate transformation for an extended inversion formula, the approach of in-

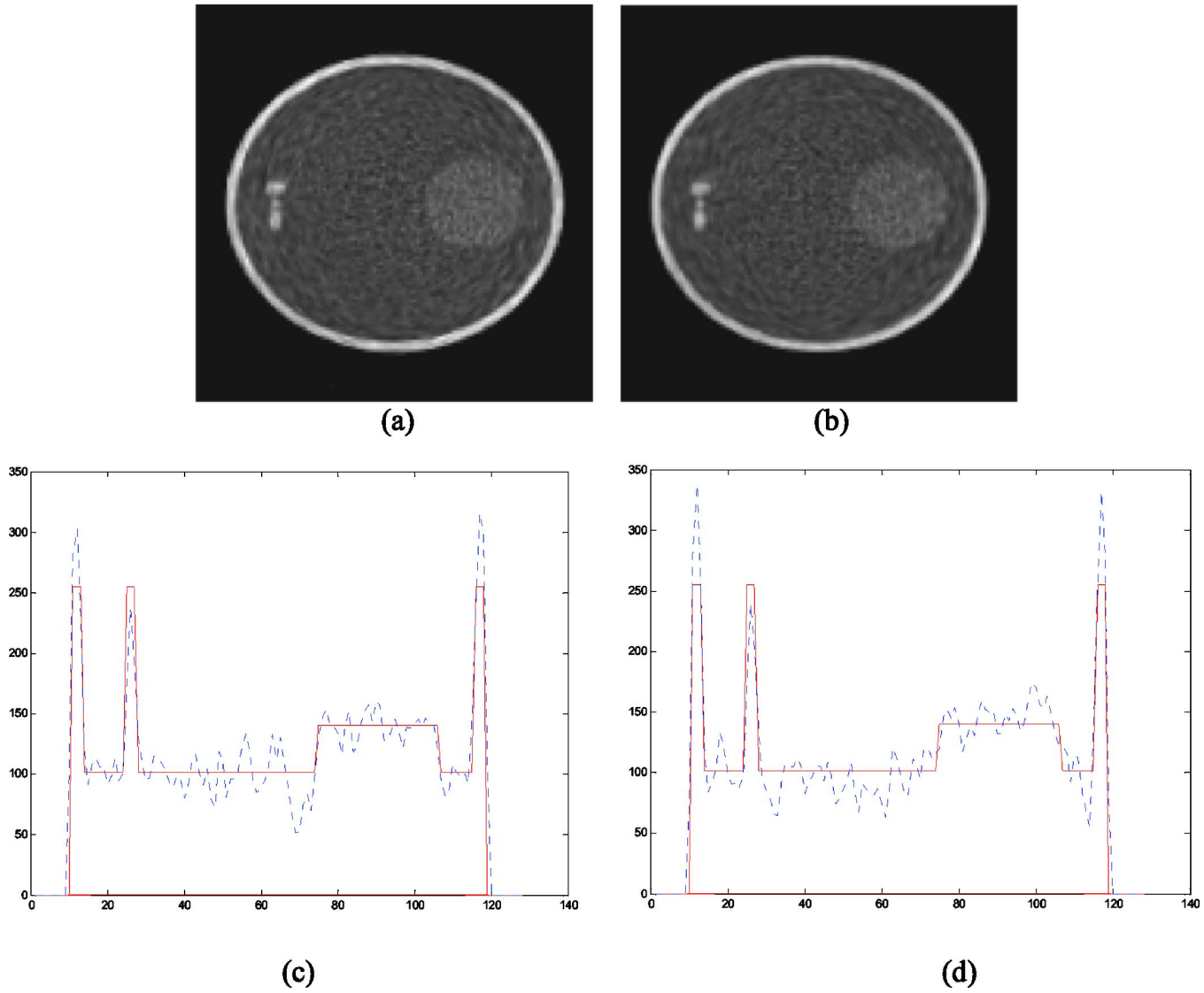

FIG. 7. Reconstructions from projection data with Poisson noise (total counts per view is 100 K). Picture (a): fan-beam reconstructed result with $D(p)=300$ pixel units. Picture (b): VFF result with $D(p)=100+10|p|$ pixel units. Picture (c): profile of image (a) along the horizontal central line (where solid line is from the phantom). Picture (d): profile of image (b) along the horizontal central line.

terpolating the projection data into parallel-beam geometry and then use of parallel-beam inversion formula to reconstruct the interpolated data is straightforward. A through comparison of these two strategies is needed.

ACKNOWLEDGMENTS

This work was supported in part by the BIT Research Foundation, NIH Grant No. CA082402, and SRF for ROCS, SEM. The authors are grateful to Dr. RoseMary N. Citrola for editing this paper.

[1]G. T. Gullberg, *The Attenuated Radon Transform: Theory and Application in Medicine and Biology*, Ph.D. dissertation, University of California at Berkeley, CA, 1979.
[2]E. Arbuzov, A. Bukhgeim, and S. Kazantsev, "Two-dimensional tomography problems and the theory of A-analytic functions," Siberian Advances in Mathematics **8**, 1–20 (1998).
[3]R. G. Novikov, "An inversion formula for the attenuated X-ray transformation," Ark. Mat. **40**, 145–167 (2002).
[4]L. A. Shepp and B. Logan, "The Fourier reconstruction of a head section," IEEE Trans. Nucl. Sci. **21**, 21–43 (1974).
[5]F. Natterer, "Inversion of the attenuated Radon transform," Inverse Probl. **17**, 113–119 (2001).
[6]L. A. Kunyansky, "A new SPECT reconstruction algorithm based on the Novikov's explicit inversion formula," Inverse Probl. **17**, 293–306 (2001).
[7]J. Wen, T. Li, and Z. Liang, "Ray-driven analytical fan-beam SPECT reconstruction with non-uniform attenuation," *Proc. IEEE International Symposium on Biomedical Imaging* (ISBI, 2002), pp. 629–632.
[8]J. You, G. L. Zeng, and Z. Liang, "FBP algorithms for attenuated fan-beam projections," Inverse Probl. **21**, 1179–1192 (2005).
[9]T. Li, J. You, J. Wen, and Z. Liang, "An efficient reconstruction method for non-uniform attenuation compensation in non-parallel beam geometries based on Novikov's explicit inversion formula," IEEE Trans. Med. Imaging **24**, 1357–1368 (2005).
[10]J. Wen, T. Li, and Z. Liang, "An analytical inversion of non-uniformly attenuated Radon transform for SPECT reconstruction with variable focal-length fan-beam collimators," IEEE Trans. Nucl. Sci. **50**, 1541–1549 (2003).
[11]Q. Huang, G. L. Zeng, J. You, and G. T. Gullberg, "A cone-beam reconstruction algorithm for non-uniformly attenuated projections acquired us-

ing a circular trajectory," Phys. Med. Biol. **50**, 2329–2339 (2005).
[12]J. Wen, Z. Wang, B. Li, T. Li, and Z. Liang, "Speed up of an analytical algorithm for non-uniform attenuation correction using PC video/graphics card architecture," IEEE Trans. Nucl. Sci. **51**, 726–732 (2004).
[13]G. L. Zeng, G. T. Gullberg, R. J. Jaszczak, and J. Li, "Fan-beam reconstruction algorithm for a spatially varying focal length collimator," IEEE Trans. Med. Imaging **12**, 575–582 (1993).
[14]G. L. Zeng and G. T. Gullberg, "A backprojection filtering algorithm for a spatially varying focal length collimator," IEEE Trans. Med. Imaging **13**, 549–556 (1994).
[15]R. J. Jaszczak, C. E. Floyd, S. H. Manglos, K. L. Greer, and R. E. Coleman, "Cone beam collimation for SPECT: Analysis, simulation, and image reconstruction using FBP," Med. Phys. **13**, 484–489 (1986).
[16]Z. Liang, J. Ye, J. Cheng, and D. Harrington, "Quantitative brain SPECT in three dimensions: An analytical approach to non-uniform attenuation without transmission scans," in *Computational Imaging and Vision* (Kluwer Academic, Dordrecht, The Netherlands, 1996), pp. 117–132.
[17]O. Tretiak and C. E. Metz, "The exponential Radon transform," SIAM J. Appl. Math. **39**, 341–354 (1980).
[18]A. Bellini, M. Piacentini, C. Cafforio, and F. Rocca, "Compensation of tissue absorption in emission tomography," IEEE Trans. Acoust., Speech, Signal Process. **27**, 213–218 (1979).
[19]T. Inouye, K. Kose, and A. Hasegawa, "Image reconstruction algorithm for SPECT with uniform attenuation," Phys. Med. Biol. **34**, 299–304 (1989).
[20]C. E. Metz and X. Pan, "A unified analysis of exact methods of inverting the 2-D exponential Radon transform," IEEE Trans. Med. Imaging **14**, 643–658 (1995).
[21]X. Pan and C. E. Metz, "Analysis of noise properties of a class of exact methods of inverting the 2-D exponential Radon transform," IEEE Trans. Med. Imaging **14**, 659–668 (1995).
[22]Y. Weng, L. Zeng, and G. T. Gullberg, "Analytical inversion formula for uniformly attenuated fan-beam projections," IEEE Trans. Nucl. Sci. **44**, 243–249 (1997).
[23]J. You, Z. Liang, and G. L. Zeng, "A unified reconstruction framework for both parallel-beam and variable focal-length fan-beam collimators by a Cormack-type inversion of exponential Radon transform," IEEE Trans. Med. Imaging **18**, 59–65 (1999).
[24]P. Dreike and D. P. Boyd, "Convolution reconstruction of fan-beam projection," Comput. Graph. Image Process. **5**, 459–469 (1976).